Turkish Journal of Civil Engineering, 2023 45-69, Paper 740, ***Research Article***

Seismic Responses of an Isolated Long-span Bridge using Frequency Domain and Time Dependent Procedures

Fevzi SARITAŞ[1]
Zeki HASGÜR[2]

ABSTRACT

Seismic behavior of an isolated bridge is analyzed in the frequency domain under the effects of non-stationary ground motions. For dynamic solutions, different ground environments are considered by simulating non-stationary quakes that can be represented from bedrock to soft ground level. In the simulations, power spectral functions and filtered white noise model are adopted for spectral densities of the earthquake excitations. Various computer algorithms have been developed for earthquake simulations, establishing the bridge finite element model and stochastic solutions. Twenty simulated ground motions are used for each soil profile and the parameters of Rayleigh dispersion are estimated by evaluating the system responses for each ensemble. A number of peak response factors dependent on soil conditions are presented for seismic responses. In addition, extreme value distributions of the responses are shown with the probability of exceeding functions and tables. The responses are discussed for the specific exceedance level of probabilities used in probabilistic design process. The stochastic analyses generally yielded responses consistent with time domain solutions. Exceedance probability functions of the peak responses were obtained in a close relationship. However, the probability distributions of the responses decomposed for the soft soil case and they displayed a wider dispersion even for low exceedance levels. The peak responses are expressed with some exceedance probabilities. In the estimation of response variations, this study showed the practicality of the frequency domain method and the results revealed higher peak response factors and variances for softer soil conditions. Furthermore, this study indicated that the frequency domain procedure is an effective tool in the obtaining of non-stationary seismic responses.

Keywords: Non-stationary, simulated earthquakes, peak responses, power spectrum, isolator.

Note:
- This paper was received on November 23, 2022 and accepted for publication by the Editorial Board on April 14, 2023.
- Discussions on this paper will be accepted by September 30, 2023.
- https://doi.org/10.18400/tjce.1208867

1 Darmstadt Technical University, Department of Civil Engineering, Guest Researcher, Germany
saritasfe@itu.edu.tr - https://orcid.org/0000-0003-0605-1450

2 Altınbaş University, Department of Civil Engineering, İstanbul, Türkiye
zeki.hasgur@altinbas.edu.tr - https://orcid.org/0000-0002-7769-5678

1. INTRODUCTION

Earthquake motions include wide range of uncertainties such as magnitudes, frequency contents, amplitudes and etc.) and non-uniform characteristics (wave passage effects, site effects, reflections during propagation, and etc.). Due to their non-stationary nature, earthquakes are very complex ground motions and they vibrate structural systems in a non-synchronous form. Therefore, they cause large fluctuations in the seismic structural responses. Spatial variation of an earthquake mainly originates from three sources; loss of coherence effects, wave passage and local soil conditions. Long span bridges are highly sensitive to quake excitations. Due to large variability, dynamic responses develop in non-deterministic manner even for the same seismic zone. Seismic response variations may be determined either by deterministic approaches assuming a set of specific ground motions in a limited number or by stochastic approaches considering random process of the ground motion. Shinzouka and Jan [1] showed that if the cross-spectral and the power spectral density function (PSDF) of a process or an ensemble are known, then its components can be simulated by the sum of trigonometric functions containing random phase angles and frequencies. The earthquake intensity could be an important guideline in estimating the dynamic responses due to an earthquake since the responses of the system increase with the intensity of the earthquake [2]. Pagnini and Solari [3] carried out frequency analysis of bridge piers by assuming stationary Gaussian process and Kanai-Tajimi filtered white noise model. Numerical results showed that the variation of the response is virtually independent of the spectral content of input motion. Der Kiureghian and Neuenhofer [4] developed multi-support response spectrum method for the seismic responses of bridges. Under effects of white noise and filtered white noise excitations, the close-form expressions were derived [5] for spectral moments of the responses. Vrouwenvelder [6] proposed a direct method to analyze bridges in frequency domain for non-uniform seismic motions. This study indicated that the design of bridges subjected to ground motions should be considered as a probabilistic problem together with risk analysis and decision mechanism. Yang and Leung [7] used stochastic finite segment method on box-girder bridges. The analysis point that the method is more effective in terms of the number of unknowns and it has higher accuracy. On the other hand, the frequency analysis may be a strong tool to exhibit larger redistribution of responses in case of non-uniform seismic motions [8].

For a single bridge pier with symmetric cantilevers, stochastic analysis was studied by Hasgür [9] and responses were evaluated in terms of statistical values. On the other hand, spatial variability of earthquakes and soil conditions may quite affect the stochastic responses of the piers of an isolated bridge [10]. Jangid [11] used non-stationary random process for earthquake excitation to obtain frequency responses of bridges by a suitable PSDF. Closed-form solutions were derived for optimum yield strength of bearings by assuming rigid-deck and stationary white-noise motion. In obtaining responses in the frequency domain, hysteretic energy dissipation procedure is also used for isolators by considering the Kanai-Tajimi model [12]. Additionally, the optimum values of the characteristic strength and inelastic stiffness of isolators depend on frequency content of ground motion and consequently depend on soil conditions as well [13]. On the other hand, seismic performance of the considered bridge and pier was evaluated [14,15] under earthquake motions. In obtaining the peak responses, the coupled interactions of restoring forces in isolators have been observed as considerable effects [16]. For peak responses, the models of peak factors suggested by Davenport [17] and Vanmarcke [18] have been commonly used so far. When earthquake damages in bridges are

investigated, pier stiffness, soil conditions and supporting types are seen as important factors. Soil flexibility can quite affect [19] the seismic responses of base-isolated structures and lead rubber isolation system (high damping) can causes to larger peak responses. From the mentioned effects, different soil mediums and support conditions were studied [20] under effect of earthquake accelerations to obtain dynamic responses of a bridge-pier system. Differences in soil conditions induce significant variations in seismic responses of bridges with high piers and more flexible soil can cause the higher seismic responses [21]. Since the seismic responses are dependent on the dynamic characteristic of the bridge and the PSD of input excitations, the model of coherency and the apparent velocity, the spatially varying ground motions play important role in the bridge analyses [22]. In suspension bridges, the response values obtained for the site-response effects alone are larger than the response values obtained for the incoherence and wave passage effects, by themselves [23].

In this study, expected peak responses of a viaduct system subjected to non-stationary earthquakes are predicted in frequency domain for different soil conditions. The spatial variability of the input motion is considered by power spectral density functions. The analyzed viaduct was constructed on a highway and it has multiple-long spans and rubber isolators located between deck and piers. The viaduct was built as a reinforced concrete structure in a high seismic zone (in Istanbul) of Turkey. For the analyses, twenty non-stationary earthquake records are simulated for each soil type by using filtered white noise model and time-varying functions which are modulated with suitable parameters fitting to the considered records. Establishing the 3D finite element model of the viaduct system, generating artificial ground motions and frequency analyses are executed by the algorithms. A range of peak response factors are presented in this paper for various soil conditions and behavior type of bearings. The expected peak responses in frequency domain are evaluated with those of the time domain and it has been shown that the results are in a harmonious relationship. Finally, the expected peak responses are computed for non-stationary earthquake effects in point of probabilistic terms such as mean, variance and etc. By extreme values analysis, exceedance probability distributions are obtained for seismic peak responses. Furthermore, the response quantities corresponding to 2%, 10% and 50% exceedance probabilities to be used in design process are predicted depending upon soil types.

2. BEHAVIOR OF THE VIADUCT IN FREQUENCY DOMAIN

Random behavior of a system can be expressed with statistical quantities and structural safety can be evaluated in terms of probability of exceedance for certain levels. As is well known, linear model of a structural system subjected to random loads is generally sufficient [24] for serviceability assessment in probabilistic sense. Different soil conditions give rise to additional variations in the amplitude and frequency content of the ground motions as the waves propagate from the bedrock to the surface level [25]. In the analysis of a system subjected to loading p(t) involving stochastic character, the main task is to transform the stochastic process of the loading p(t) into the random processes of the response by employing proper mathematical techniques for frequency domain solution as shown by the simplest description given in Figure 1.

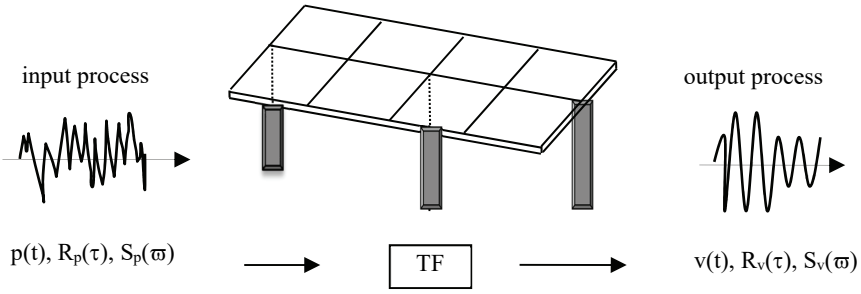

Figure 1 - Input and output in a random process

The stationary process of the loading p(t) can be regarded as an input function provided that one of either the autocorrelation function $R_p(\tau)$) or the PSDF ($S_p(\varpi)$) is known. In order to consider the randomness of ground motions, it is assumed that the external load p(t) representing non-stationary random process has a limited frequency band, zero-mean value and a Gaussian distribution with uniform power spectral intensity of So. The response process v(t) can be defined by integration of the multiplication of the transfer functions (TF) and Fourier spectrum of seismic input. Equations of motion for a multi-degree of freedom (MDOF) system are defined for ground motion of by:

$$[m]\{\ddot{v}\} + [c]\{\dot{v}\} + [k]\{v\} = \{p_{eff}(t)\} = -[m]\{1\}\ddot{v}_g \quad (1)$$

The terms [m], [c] and [k] represent the mass, damping and stiffness matrix of the system, respectively. Vectors $\{\ddot{v}\}$, $\{\dot{v}\}$ and $\{v\}$are the acceleration, velocity and displacement, respectively. By applying inverse Fourier transforms to the frequency-based response of the system, the modal response in its n^{th} normal mode is,

$$Y_n(t) = \frac{1}{2\pi}\int_{-\infty}^{+\infty} H_n(i\varpi) \rightleftarrows \ddot{V}_g(i\varpi)e^{i\varpi t}d\varpi \quad (2)$$

where $H_n(i\varpi)$ is the complex frequency response function, n=1,2, …, N $\ddot{V}_g(i\varpi)$ and is the Fourier transformation of the input motion. The complex frequency response function for a discrete mode of n is given [26] as follows,

$$H_n(i\varpi) = \frac{1}{K_n[1+2i\xi_n(\varpi/\omega_n)-(\varpi/\omega_n)^2]} \quad (3a)$$

$$H_n(-i\varpi) = \frac{1}{K_n[1-2i\xi_n(\varpi/\omega_n)-(\varpi/\omega_n)^2]} \quad (3b)$$

K_n denotes the generalized stiffness matrix for the n^{th} mode. Modal responses for stationary random ground motions can be expressed by a stochastic process of the generalized discrete forces. Knowing the cross spectral density function ($S_{VmVn}(\varpi)$) defined for discrete modal forces P_n and P_m, any response of v(t) is obtained by superposing the frequency response functions as follows:

$$\sigma^2_{v(t)} = \sum_m \sum_n D_m D_n S_{P_m P_n} \int_{-\infty}^{+\infty} H_m(i\,\varpi) H_n(-i\varpi) d\varpi \quad (4)$$

The above function shows a relationship between the input and the output processes and it states the variance of any response quantity. For zero-mean Gaussian process, the relation in Eq. (2.4) yields the mean-square responses. $H_m(-i\varpi)$ and $H_n(-i\varpi)$ are the complex conjugate of the $H_m(i\varpi)$ and $H_n(i\varpi)$, respectively. The coefficients D_m, D_n, E_m and E_n are expressed in terms of the modal parameters and obtained by standard structural analysis. Total behaviour is derived on the basis of modal superposition by using these coefficients (D_m, D_n, E_m, E_n) expressing the contributions of mode shapes. The solution vector associated with normal coordinates is obtained by multiplication of any response quantity with these coefficients. For each mode, these coefficients are obtained by any response dividing to the value of normal coordinate.

When the contribution of the cross terms to the mean-square responses is considered for discrete modal frequencies, the variances of the output process are computed via numerical integrations of Equation (4) by applying the residue integration method. Thus, the variances of response quantities in terms of bending moments and shear forces are given by:

$$\sigma^2_M = \sum_m \sum_n \frac{4\pi\xi\omega_m^2\omega_n^2 D_m D_n S_{P_m P_n}}{K_m K_n(\omega_m+\omega_n)[(\omega_m-\omega_n)^2+4\pi\xi^2\omega_n\omega_m]} \quad (5)$$

$$\sigma^2_V = \sum_m \sum_n \frac{4\pi\xi\omega_m^2\omega_n^2 E_m E_n S_{P_m P_n}}{K_m K_n(\omega_m+\omega_n)[(\omega_m-\omega_n)^2+4\pi\xi^2\omega_n\omega_m]} \quad (6)$$

3. DEFINITION OF GROUND MOTION

Ground motions having non-stationary character are assumed to be stochastic processes and the response of the system is defined by the functions between the input and the output process of the system. The power spectrum of Kanai-Tajimi filter functions can be defined [27] as a variation of the characteristics of ground motions arising from the bedrock passing through soil layers. Stochastic approach may be the most suitable procedure for generating artificial accelerograms for the reason of the complex nature of the formation of seismic waves, their travel path before reaching the recording station and local soil conditions at the site. In this regard, different stochastic models, both stationary and non-stationary, have extensively been used in the literature to simulate earthquake ground motions. Firstly, stationary white noise random models were developed for modeling of earthquake ground motions. In this context, stationary filtered white noise model of Kanai–Tajimi ([28], [29]) has been the preferable model for many researchers and engineers. These efforts were followed by introduction of the non-stationary stochastic models for generating earthquake accelerograms ([30], [31]). In the simulation of ground accelerations, stationary white noise type ground motions are necessarily considered together with filter functions to characterize the variations in different soil environments. Kanai- Tajimi filters and later improved/modified by Clough and Penzien [32] are well-known and commonly used functions. The Kanai-Tajimi filter ($|H_g(i\varpi)|$) ampflies the high-frequency components and de-amplfies rapidly the low frequencies. The Kanai-Tajimi filter (high-pass) is used to define bedrock ground accelerations and it prevents the transition of very low frequency components

originating from bedrock. This case can yield inappropriate structural responses. Therefore, to eliminate this difficulty, a second filter function, known as Penzien's filter function (low-pass, $|H_f(i\varpi)|$), is adopted to enable the transition of very low frequency components. Random process of the earthquake excitations is defined by filtered white noise in the stochastic analyses. PSDF of a sampled random process of x(t) filtered by the transfer functions is considered as,

$$S_x(\varpi) = \left|H_g(i\varpi)\right|^2 \left|H_f(i\varpi)\right|^2 S_0 \qquad -\infty < \varpi < +\infty \tag{7}$$

where the constant power spectral intensities (S_o) are evaluated for each soil type in the numerical analyses. The corresponding filter functions of the $|H_g(i\varpi)|$ (high pass filter) and $|H_f(i\varpi)|$ (low pass filter) are given by

$$\left|H_g(i\varpi)\right|^2 = \frac{1+4\xi_g^2(\varpi/\omega_g)^2}{[1-(\varpi/\omega_g)^2]+4\xi_g^2(\varpi/\omega_g)^2} \tag{8}$$

$$\left|H_f(i\varpi)\right|^2 = \frac{(\varpi/\omega_f)^4}{[1-(\varpi/\omega_f)^2]^2+4\xi_f^2(\varpi/\omega_f)^2} \tag{9}$$

where ω_g and ξ_g parameters are ground circular frequency and ground damping ratio, respectively. The second filter characteristics of ω_f and ξ_f modify the shape of power spectrum at very low frequency values. Kanai suggested 15.6 rad/sec for the characteristic ground circular frequency and 0.6 damping ratio for hard soil type. For various soil types, the parameters of ξ_g and ω_g used in this study are given by literature study [4]. Other filter parameters are taken into account by ξ_f=0.60 and ω_f=ω_g/10. In this study, the power spectrum of each soil type is calculated by using Parseval theorem [33] and Fast Fourier transforms. The amplitudes of the process are directly obtained for each sample by the area under curve of $S_x(\varpi)$. This curve is considered by equal frequency interval of $\Delta\varpi$ and the random phase angle of φ_{kr} which has uniform probability density function over the range of $0<\varphi_{kr}<2\pi$ with intensity of $1/2\pi$. In initial region of records, acceleration amplitudes generally develop with an increase tendency up to a maximum level. After following a region assumed as constant, acceleration traces decrease rapidly and then show little changes in the tail section. In defining of a filtered process with non-stationary character, the duration characteristics of t_1, t_2, t_3, t_4 and the constants of μ and k are studied [34]in detail by Jennings et al. Earthquake response spectra and the power spectral density functions are simulated for the expected earthquakes by applying the given procedure.

4. SIMULATION OF EARTHQUAKE MOTIONS

Almost five decades ago, the pioneers of the earthquake engineering such as Housner and Jennings [35] studied generation of artificial ground motions by using random process. After the generation of earthquake ground motions, response and ductile spectra were studied and investigated with for the purpose of non-stationary amplitudes and frequency content of motion by Hasgür [31]. Şafak et al.[36] presented a model to characterize and to simulate ground motions by including white noise and squared accelerations. Wavelet method is an

alternative technique [37]in generation motions by using variations of amplitudes, frequency content and phase-angle. In this study, the most compatible parameter-values for the time-modulated function z(t) are obtained by using proper approaches. The non-stationare nature of the actual acceleration traces can be seen from a general process. As is discussed above, the acceleration amplitudes that tend to increase up to peak level occur generally within a small range from the beginning of the quake. Following this specific interval, peak amplitudes appear during the effective duration (t_{eff}) and then acceleration traces decrease exponentially in tail part. From this point of view, the filtered process having non-stationary form is obtained by applying an envelope function of z(t) as given in Figure 2a. The curve of z(t) is specified according to the statistical analysis of the real acceleration traces reflecting the seismic zone characteristics. In calculation of the parameters of z(t), t_1 and t_2, normalized Arias intensity and effective durations (t_1, t_2) are utilized. In the simulation of accelerations, the regression coefficients for the exponential functions are evaluated iteratively by the trial-and error method. In the simulations, k=2.951 and μ=0.1665 are computed values for the envelope function. The parameters of t_1 and t_2 are considered as 2.3 sec and 6.5 sec, respectively.

For analyses, twenty ground motions are generated for various soil types (hard, mild and soft) and bedrock level by using recorded motion of the 1992 Erzincan-NS-component which has largest Housner's spectrum intensity ($SI_{0.2}$). For the considered seismic zone, this parameter may be used as an instrumental intensity to define destructiveness of an earthquake.

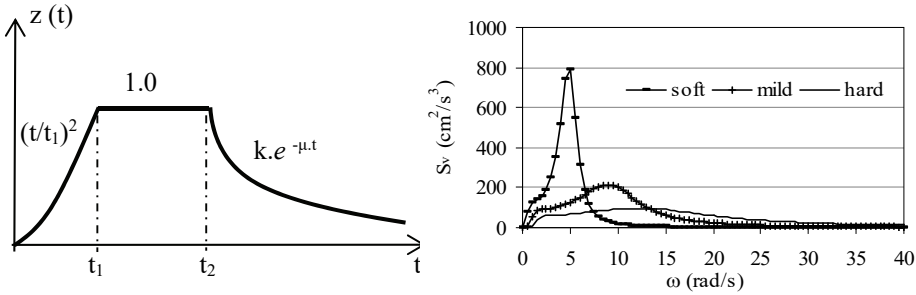

a) Time-modulated function *b) Filtered power spectra*

Figure 2 - Time-modulated function and filtered power spectra

The constant power spectrum intensities are computed depending on soil types as well as for the smoothed curves of El Centro NS 1940 record [38]. To compare the parameters of the PSDFs, the same process is implemented for Erzincan NS 1992 earthquake and the results for both records are given in Table 1.

Thus, the smoothing- process has no considerable influence over the power intensities. Numerical integrations of PSDF of the El Centro and Erzincan earthquakes are obtained as 0.4726 m^2/s^4 and 0.4875 m^2/s^4, respectively. The product function of $\Phi i(\varpi)$ is introduced here over the frequency limit of s (49.95 Hz) and given for each soil type by the following relation:

Table 1- Constant power spectrum intensities

a) El Centro NS 1940 NS record

Soil type	**Φ_i** (rad/s)	**S_o**(cm^2/s^3)	**$S_o^{smoothed}$**(cm^2/s^3)
hard	46.08	51.24	51.16
mild	31.50	74.95	74.84
soft	22.57	104.62	104.45

b) Erzincan NS 1992 record

Soil type	**Φ_i (rad/s)**	**S_o(cm^2/s^3)**
hard	46.08	52.91
mild	31.50	77.40
soft	22.57	108.04

$$\Phi_i(\varpi) = \int_0^s \left|H_g(\varpi)\right|^2 \left|H_f(\varpi)\right|^2 d\varpi \tag{10}$$

The power spectra of the three soil types are obtained as given in Figure 2b. A high spike is clearly seen in the soft soil in compared to other power spectra. In Figure 3, the response spectra of the 20 simulated accelerations are presented depending upon periods for each soil type. As expected, the peak spectral values are appeared in a wide-interval at higher periods for the soft soil type. To perform an assessment, the simulated 5 percent damped response spectra are also illustrated comparatively with design spectrum given by Turkish earthquake code (TSEC, 2019). There are some differences between the simulated and the design response spectra, because the simulated spectra are generated based on the power spectrum density function of a recorded ground motion and the simulated ground motions are filtered out by different types of filter functions given in the literature as mentioned above.

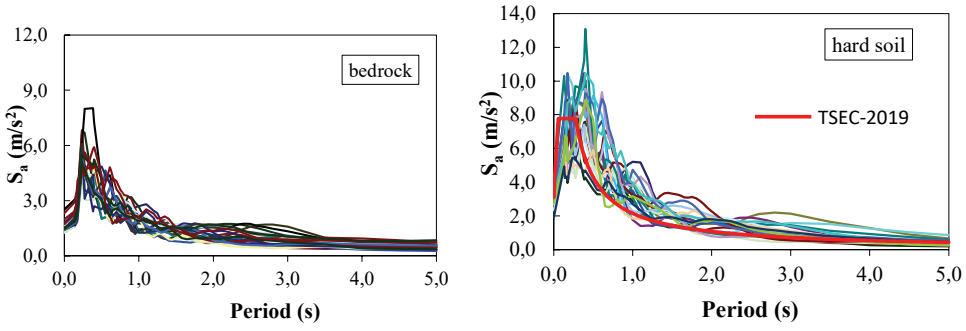

Fig. 3a - Generated response spectra for different soil conditions

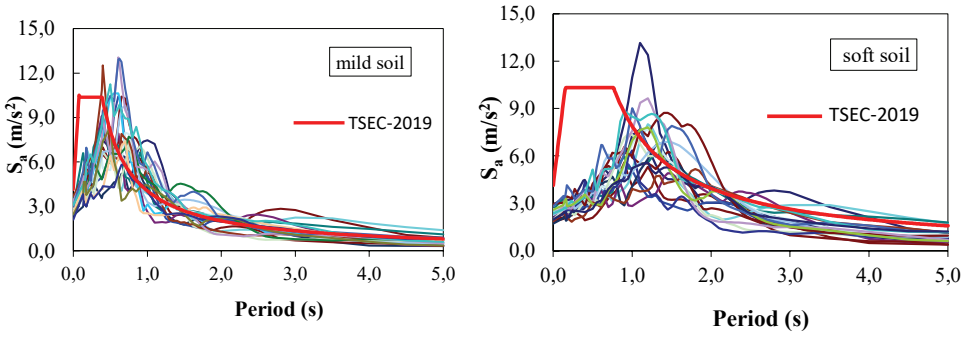

Fig. 3b - Generated response spectra for different soil conditions (5 percent damped)

Furthermore, the response and power spectra are comparatively given in Figure 4 for the recorded (Erzincan NS 1992, 5 percentdamped) and the mean of the simulated motions. When the consistency of the results is investigated, it is seen that the simulated power and the acceleration spectra show good accuracy. It means that the simulated ground motions can represent the expected ground motions for the considered zone. Since the simulated acceleration and the power spectra are close to those of the recorded ones in acceptable level of accuracy, it is decided to employ the simulated records in the stochastic dynamic analyses.

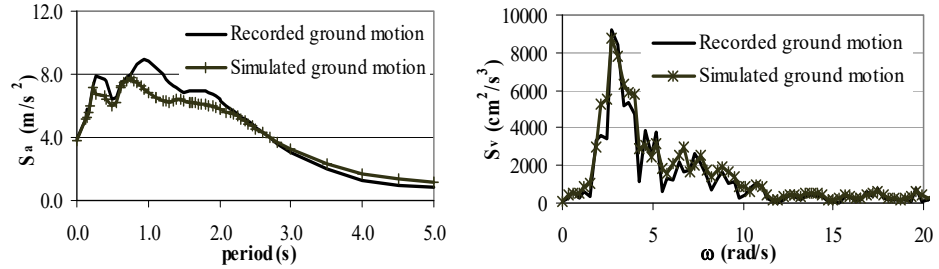

a) response spectra b) power spectra

Fig. 4 - Consistency of the simulated and recorded ground motions

5. FINITE ELEMENT MODEL AND VIBRATIONS OF THE VIADUCT SYSTEM

A multi-span viaduct system with total length of 325m is analyzed for stochastic dynamic responses. It consists of continuous deck over box-girder (V-shape), laminated rubber bearings (with steel plates) and pier with a hollow rectangular section. The viaduct has 6 spans and the maximum pier height and span length are 29.1m and 58.2m, respectively. The elevation of the viaduct, the configuration of bearings and the piers having variable cross-sections are given in Figure 5. Discretization over the system in 3D is carried on the nodal points with different mesh intervals by using finite frame elements having 12 degree of freedoms (DOF). In the finite element model (Figure 5), smaller mesh-intervals are selected

in the regions close to the piers where the variation of the cross-section takes place. Distributed mass of the system is lumped on the discrete nodal points. Equations of equilibrium of the viaduct system are formed by considering the nodal forces of the lumped mass system. Establishing finite element model (with desired mesh intervals) and performing analyses are realized by the developed software of Finite Element Analysis (FEA) as well.

Dynamic stiffness matrix corresponding to the whole viaduct system is obtained in dimensions of 786×786. Static condensation is executed on the dynamic stiffness matrix to get a simplified equivalent system. Depending on DOFs of the selected nodal points, the new reduced dynamic stiffness matrix is found to be of 78×78.For rubber bearings, bilinearized model is considered for nonlinear hysteretic behavior as given in Figure 6. K_e, K_p, K_{eff}, and

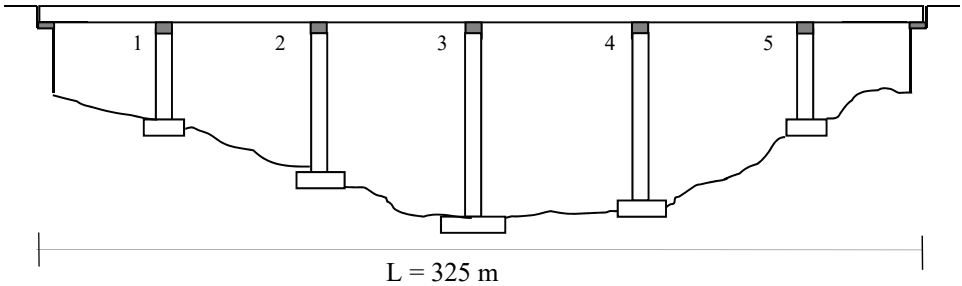

a. elevation of the viaduct system

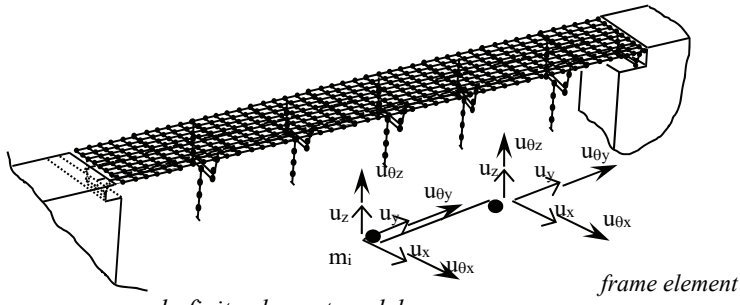

b. finite element model

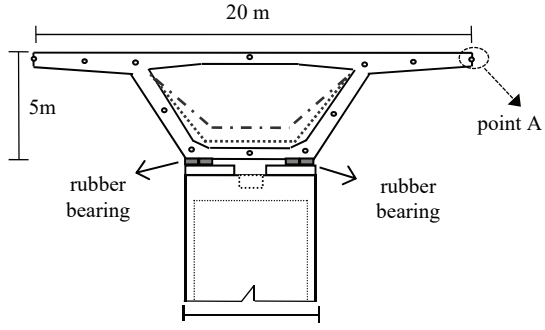

c.cross-section of the pier-deck system

Figure 5 - Elevation and cross-section of the viaduct

F_y are the initial stiffness, post-yield stiffness, effective stiffness and yielding force, respectively. K_{eff} represents hysteretic behavior of the rubber bearing. The bearing stiffness are obtained by following equations:

$$K_{eff} = K_p + \frac{Q}{\Delta} \quad (\Delta > \Delta_y) \tag{5.1}$$

$$K_p = G.\frac{A}{\Sigma t_r} \tag{5.2}$$

$$K_v = E_c.\frac{A}{\Sigma t_r} \tag{5.3}$$

where Δ is displacement of rubber bearing and Δ_y is yielding displacement. The parameter Q represents the characteristic strength and K_v is the vertical stiffness. G is the shear modulus of the rubber and A is the area in plan. $\sum t_r$ represents the total rubber thickness of a bearing. The lateral, vertical and rotational stiffness of the bearings are taken into consideration in three directions as equivalent linear stiffness. In general, rubber bearings are also designed for shear deformations and these deformations are limited with strain levels up to approximately 200 percent percent. For the isolator displacement capacity, the shear strains have been restricted by the value of γ=0,70 [39]. In case of severe dynamic vibrations, the behavior of isolator system may differ from linearity and approximate methods such as linearization techniques can be iteratively used to consider variations in isolator rigidity. The coefficients of stiffness matrices are computed based on the mechanical properties of the installed bearings. For this purpose, the relations as specified in the codes AASHTO [40], DIN 4141-14 [39] and essentials given [41] by Naeim and Kelly are utilized.

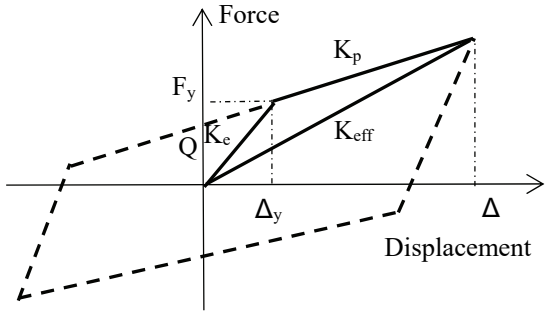

Fig. 6 - Bearing behaviour model

In order to check the validity of the developed algorithm of FEA (Finite Element Analysis), the deck-displacements of the viaduct system are evaluated under effects of seismic loads and verified with the results of a software package [42]. The lateral displacements of some nodal points on the deck are comparatively given in Table 2. From the free vibration analysis, the first four free vibration periods are obtained by FEA for two directions and the results are comparatively given with those of SAP2000 in Table 3. Since the free vibration analyses of the both real and equivalent viaduct system yield acceptable results, dynamic stiffness matrices of the equivalent model and the algorithms mentioned are adopted to use in the stochastic dynamic analyses.

Table 2 - Deck lateral displacements

	δ_x (m)	
Node	**FEA**	**SAP2000**
5	2.96×10^{-2}	2.98×10^{-2}
119	7.94×10^{-2}	8.14×10^{-2}
253	1.36×10^{-2}	1.40×10^{-2}
387	1.75×10^{-2}	1.81×10^{-2}
521	1.88×10^{-2}	1.93×10^{-2}
655	1.72×10^{-2}	1.75×10^{-2}
775	1.49×10^{-2}	1.50×10^{-2}

Table 3. Free vibration periods of the viaduct system

	Lateral periods (sec)			
System matrix	T_1	T_2	T_3	T_4
FEA-786×786	1.865	1.548	1.081	0.622
FEA-78×78	1.903	1.574	1.095	0.620
Sap2000	1.884	1.560	1.090	0.625

	Vertical periods (sec)			
System matrix	T_4	T_5	T_6	T_7
FEA 786×786	0.330	0.303	0.300	0.285
FEA 78×78	0.379	0.365	0.352	0.341
Sap2000	0.347	0.329	0.308	0.291

6. RESPONSE OF THE VIADUCT SYSTEM

Under effects of the generated non-stationary motions, input excitations and outputs of the structural system are computed on the basis of soil types and rubber behavior model as well. Although the viaduct piers having isolators are assumed as in the elastic range under the considered seismic forces, but influences of the nonlinear behavior of the isolator are only deterministically studied. While an isolation system reduces the earthquake effects, on the other hand it tries to keep [11] the behavior of the structure within elastic limits. Additionally, the statistical parameters of the peak responses are evaluated at the points where may be critical for the system. For a process having zero-mean, root mean square (rms) value yields standard deviation and expected mean peak responses can be obtained by way of maximum response factor which is defined as a ratio of maximum response to standard deviation. Under effect of non-stationary excitations, the peak response factors are calculated for base responses (shear forces, moments) by damping ratio of 5 percent. The variations of these

factors are obtained for the piers situated in half of the system given in Figure 7(a, b) for each soil type. For the responses at the base of piers, the peak factors are obtained in the range of 3.08~3.29 for bedrock, 2.89~3.18 for hard soil, 2.91~3.24 for mild and 2.97~3.11 for soft soil. The peak factors of the abutments develop higher than those of the interior piers. For displacements, these factors appear in range of 2.88~3.04. Generally, the lowest quantities are found for soft soil condition. As it is seen from the figures, the ranges for shear forces and bending moments are almost the same because they are base responses of the same nodal point. For a three-span suspension bridge (770 m in length) considering partially correlated stationary ground motions, peak factors were found[42] in the range of 2.81~3.22 for span moment, displacement and cable tension. Nonlinear behavior of a system having long spans is expected to occur in most severe earthquakes and it may cause significant effects on the seismic responses. However, elastic behavior, as expected in case of moderate or medium earthquakes, is essentially adopted to overcome the difficulty in the frequency domain solutions.

If the response results are examined with regard to soil medium, the stiffer soil condition yields also larger peak factors. Under effect of the simulated motions, the expected peak responses of the middle pier and an interior pier are separately obtained for 5 percentpercent damping ratio. The mean values of peak base responses (shear force and bending moment) are comparatively also presented in Figure 7 for each soil type by considering frequency and time domain solutions. The response comparisons are illustrated for the piers located at mid-span and 2nd pier. The solutions in frequency domain are obtained by assuming an equivalent constant intensity for each power spectrum. From the figures, it is observed that the solutions obtained in frequency domain are lower than those of the time domain for each soil type and therefore the highest mean values for peak responses appear in time domain solutions (especially in spectral solutions). Whereas the stochastic solutions mostly yield compatible results in acceptable level with reference to the time history quantities, large differentiations are observed for the soft soil case.

As the rigidity of the soil medium increases, the differences in response values become larger in terms of the solution methods. For example, the results of hard soil are seen as much more compatible than those of the soft soil. On the other hand, the soft soil condition may cause significant variations in responses and large differences especially for bending moments. It should be noted that while the time domain results are achieved by realizing a great number of solutions for each soil type, the frequency domain results are directly computed by considering PSDF intensities of the motion considered. The reason of the differences between the stochastic and time domain methods mainly arises from theoretical basis of the approaches. Although time domain results are specific for each record, the results of stochastic analysis are obtained as general solutions for the expected earthquake.

The variations in mean peak values and variances of the pier-base responses are shown for along the viaduct system in Figure 8. Whereas the mean peak responses exhibit similar lines in terms of soil variability, distinct increases in mean values and variances of the responses are observed for soft soil type as shown in figures. While the highest variances of the peak responses are observed in the soft soil for all cases, the lowest variances appear in case of bedrock and hard soil as expected. The soft soil case showed relatively large variations due to its amplifications which depend on filter parameters of the waves in the soil medium.

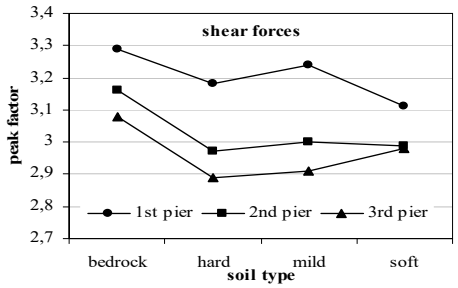

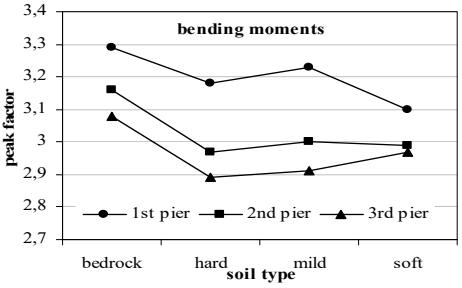

a) peak response factors for shear forces *b) peak response factors for bending moments*

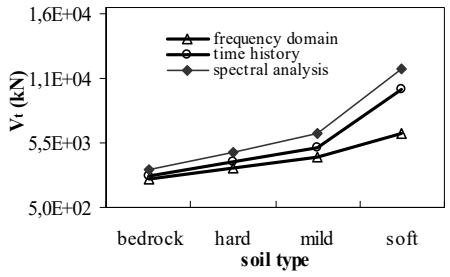

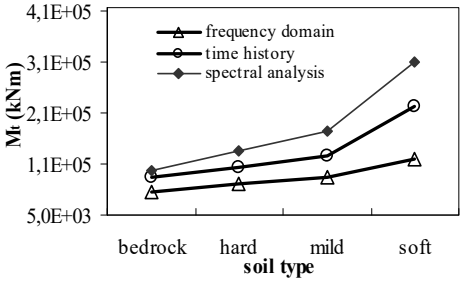

a) expected shear forces (midspan- pier) *b) expected bending moments*

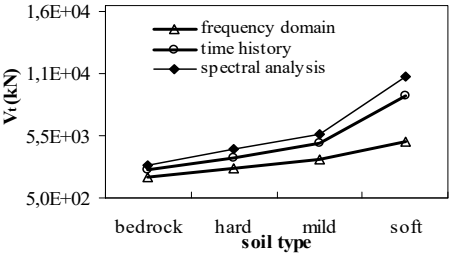

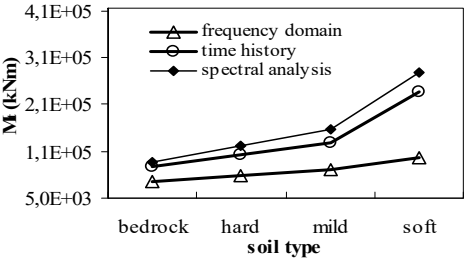

c) expected shear forces (2nd-pier) *d)) expected bending moments*

Figure 7 - Peak response factors and expected mean-peak responses for soil types with solution methods

It is derived that the peak values of the soft soil condition increase up to about 2.4 times and variances increase up to about 7 times with reference to the values of the hard soil. The lowest variances and mean values come into being at the first pier (no:1) which has the highest rubber rigidity and it is one of the shortest piers. It is already known that these are the primary properties to limit of a viaduct system. The deck displacements are studied under the effects of the non-stationary ground motions as well. The expected mean peak displacements and variances at the points of each deck-mid-span and pier upperends are given for various soil conditions in Figure 9. The similar tendencies are observed for deck displacements and variations appear nearly in symmetric shape except for soft soil ones. The soft soil case produces very large scatter for response variations.

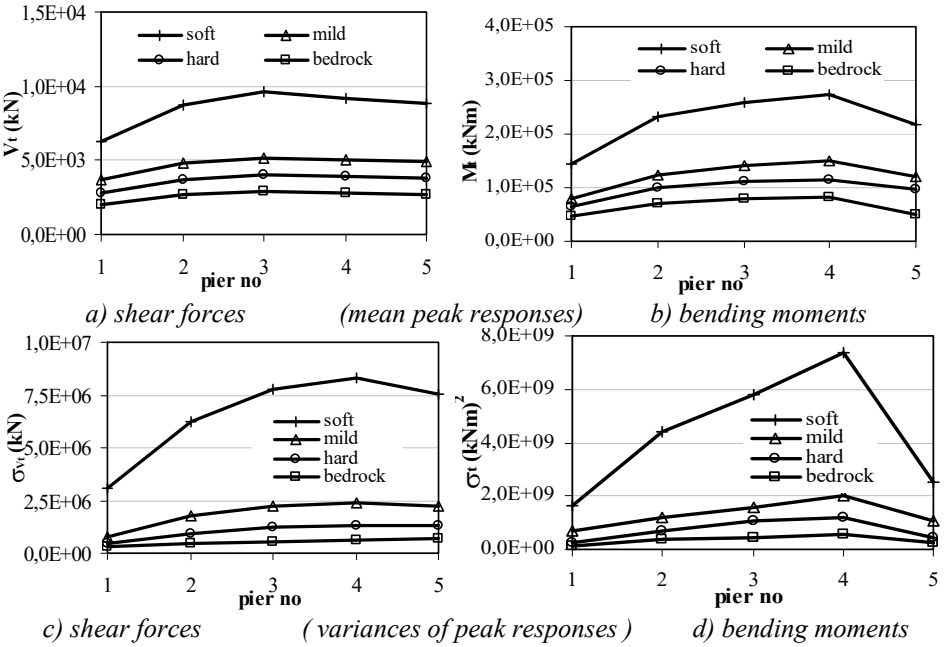

a) shear forces (mean peak responses) b) bending moments

c) shear forces (variances of peak responses) d) bending moments

Figure 8 - Peak responses of the viaduct piers

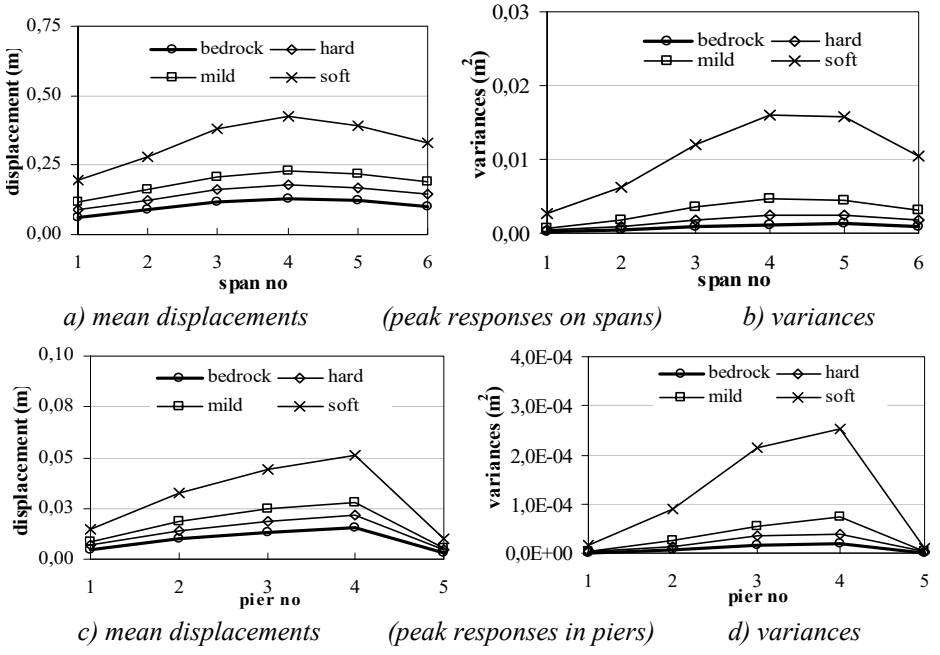

a) mean displacements (peak responses on spans) b) variances

c) mean displacements (peak responses in piers) d) variances

Figure 9 - Expected peak displacements and variances in pier upper-ends along each mid-span

While the highest displacements of the viaduct appear in the neighborhoods of mid-span, the lowest variances are observed in exterior spans for the stiff soil types. Furthermore, the fourth pier, where the highest variances are observed, is the longest column. From the figures, the soft soil condition has much more influence on the displacements than the effects of heights of the piers and bearing stiffness. Large differences between in the response values of the piers and deck indicate that the mechanical properties of the rubber bearings and the pier heights significantly affect the lateral displacement configuration of the bridge. This fact indicates that the peak responses and variances can be limited or controlled by providing soil stiffness, modifying the rigidity of bearings or designating lengthy of piers.

7. EXTREME VALUE ANALYSIS FOR NON-STATIONARY RESPONSES

The peak responses obtained in previous sections are handled herein with a distribution model and safety of the response is expressed by exceedance probability functions. For this purpose, the peak responses are assumed to follow the Rayleigh distribution under effects of earthquake excitations. Since the simulated earthquakes are considered in non-stationary form, the responses would appear in a broad interval and their confidence range cannot be easily defined. Therefore, the scatter of the responses obtained from the analyses is relatively large. This fact indicates that when a relatively high safety factor is required for ordinary structures, it cannot be accomplished economically. Deciding on the acceptable level of safety is a reasonable approach but it is an extremely complex-task. However, ductility demand can be used[43] as a design parameter in nonlinear behavior by assuming acceptable risk for a certain level of exceedance. In the present study, various exceedance probabilities are considered to evaluate the extreme responses. Since twenty non-stationary earthquakes are used for each soil type, the parameters of the Rayleigh distribution[44] values are estimated by evaluating of the system responses for each ensemble.

The mean value ($\bar{x}$), the standard deviations (σ_x) and the distribution parameter (α) of the peak displacements are given in Table 4 for the cantilever-beam end points (Figure 5, point A) on the middle-pier. The probability distributions and the exceedance probability functions derived from the extreme displacements are drawn in Figure 10(a, b) based on the soil types. The shapes of probability functions of hard and mild soil are to be similar due to close standard deviation values are to be similar due to close standard deviation values. However, the probability distributions of the soft soil display larger dispersions over a wide-interval because of quite high standard deviation and scale parameter.

Table 4 - Statistical parameters of the peak displacements

Soil type	$\bar{x}$ **(m)**	σ_x **(m)**	α
S1 (hard)	0.173	0.048	0.127
S2 (mild)	0.225	0.064	0.165
S3 (soft)	0.416	0.121	0.306

Whereas the highest exceedance probabilities yield the close peak displacement values for all soil types, the response values of the soft soil significantly decompose with larger values in low risk levels. In other words, as the exceedance probabilities decrease, the extreme displacements of soft soil case distinctly increase compared to other soil cases. Likewise, the extreme values of the base shear forces (V_t) and the overturning moments (M_t) are evaluated for some exceedance levels and they are comparatively given in Figure 10 (c, d). From the figures, the expected peak responses of soft soil case are observed with exponentially increasing values as the exceedance probabilities decrease. Namely, the similar behavior is observed for the base responses as well.

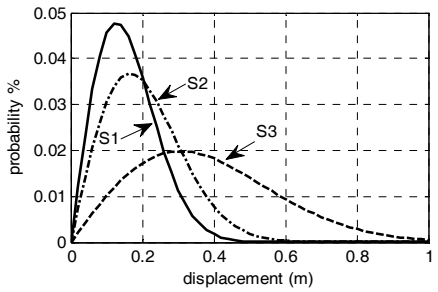

a) probability distribution functions

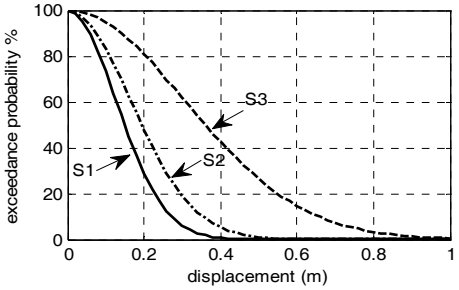

b) exceedance probability functions

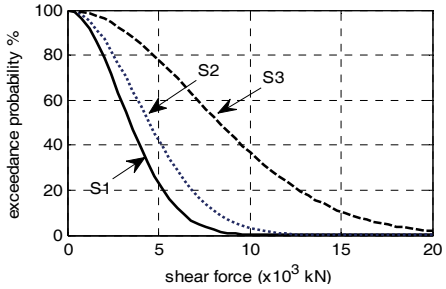

c) exceedance prob. functions for shear force

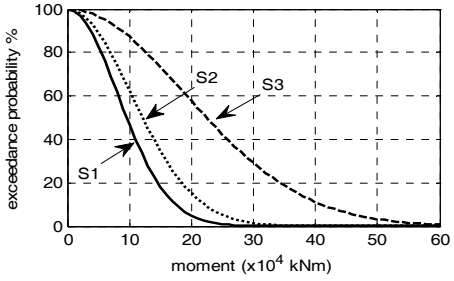

d) exceedance prob. functions for moment

Figure10 - Probability distributions for peak displacements and forces

Table 5 - Peak displacements (m) for exceedance probabilities

Soil type	Exceedance level		
	2 percent	10 percent	50 percent
S1	0.355	0.272	0.149
S2	0.462	0.354	0.194
S3	0.856	0.657	0.360

The expected peak displacements of the deck are computed depending on various exceedance probability levels (2 percent, 10 percent, 50 percent) that can be used in design codes. The corresponding displacement values are shown in Table 5. The displacements for the soft soil case yield much higher values with decreasing exceedance probabilities. Additionally, corresponding peak base responses (shear forces and moments) are obtained for the considered risk levels as given in Table 6.

Table 6 - Peak base responses for exceedance probabilities

	V_t (kN×10^3)			M_t (kNm ×10^4)		
Soil type	2%	10%	50%	10%	50%	90%
S1	8183	6278	3444	22,72	17.43	9.56
S2	10649	8170	4483	28,82	22.11	12.13
S3	19774	15170	8323	53.41	40.97	22.48

In case of very strong ground motions corresponding low exceedance probability level (2 percent), the isolation system would most likely yield and then behave in nonlinear form due to changing stiffness characteristics. Therefore, the structural solutions would require inelastic behavior model for isolation system. In this case, the solutions in frequency domain would be more sophisticate and closed-form solutions cannot be applied. Consequently, analytical/approximate techniques or discrete numerical simulations iteratively should be utilized to consider nonlinearity. It should be noted that these complex solutions require numerous and troublesome computations. In order to calculate the 2 percent exceedance probability of the system outputs, it is necessary to obtain the two important parameters (shear force and bending moments) by formulas with the given statistical variances. These values are therefore expressed. For linear behavior, it can be recommended to use the isolators by taking the displacement limits from the relevant codes. In this study, it is assumed that nonlinear behavior of the isolators cannot be allowed.

In order to obtain dimensionless values, the peak responses expressed with some exceedance probabilities are normalized by the values of the hard soil case and mean response. Thereby, the increase ratios in seismic responses are given by deterministic values for each soil conditions and exceedance levels. For the base moments normalized by the values of hard soil (Table 7), the increase ratios in the peak response values are computed as 1.269 for mild soil and 2.351 for soft soil condition. If the peak responses are normalized by expected mean values, the increase ratios are computed as shown by Table 8. The results indicate that when the exceedance probability decreases from 50 percent to 2 percent, the peak displacements increase about 2.38 times. On the other hand, the peak displacements of the exceedance probability of 10 percent increase about 1.82 times with respect to expected mean value. As it is seen from the tables, the increase ratios are independent from soil conditions.

If the peak responses are normalized by expected mean values, the increase ratios are computed as shown by Table 8. The results indicate that when the exceedance probability decreases from 50 percent to 2 percent, the peak displacements increase by a factor of about 2.38. On the other hand, the peak displacements of the exceedance probability of 10 percent

increase about 1.82 times with respect to expected mean value. As it is seen from the tables, the increase ratios are independent from soil conditions. Furthermore, it is observed that the ratios of the peak responses corresponding to any two exceedance levels are virtually same for all type of the responses. This fact yields that when the increase ratios of any soil type are known, then the extreme response values of other soil types can be predicted by using the increase ratios corresponding to any exceedance level.

Table 7 - Ratios normalized by hard soil values

Soil type	Shear force		
	2%	10%	50%
S1	1.000	1.000	1.000
S2	1.301	1.301	1.302
S3	2.416	2.416	2.416

Table 8 - Ratios normalized by median values Rewrite table

Soil type	Displacement 2%	Shear force 10%	Moment 50%
Hard	2.375	1.823	1.000
Mild	2.376	1.823	1.000
Soft	2.376	1.823	1.000

The soil-structure interaction effect was not considered. Simulated earthquakes are created based on the predominant frequency and damping factors of the ground properties. Since this study focuses on the stochastic earthquake response of the bridge for different ground conditions, the actual foundation and ground contour were not modeled for simulations. The study, which was based on the dimensions of a real viaduct, involves substantial simulations and dynamic analysis calculations that required a lot of computer processing time and memory. Depending on some parameters, a specific research topic that will cover foundation and ground interaction could be addressed in the near future.

Although calculations are made according to linear and nonlinear solution assumptions based on the equality of displacements, nonlinear time history analysis is applied as a solution type, and in the case of plastic behavior; of course, different results are obtained compared to the solution results in the linear elastic frequency domain. In terms of the difference of calculation methods, the same results cannot be expected for the bridge or viaducts due to energy consumption such as the formation of plastic hinges which are very important under nonlinear behavior. Especially in this study, the viaduct, which is considered as an example, is the approach structure to a very important suspension bridge. The performance level in the regulations foreseen as the design philosophy is the possibility of exceedance 2 percent during 100- years of economic life and very limited damage in an earthquake with $M_s \geq 7$. Immediately following the earthquake, it is expected to be opened to service. Therefore, it is

aimed to keep the ductility demand below the ductility capacity. For this reason, bridge behavior is expected in the elastic region by using auxiliary seismic isolation equipment in both design earthquakes and severe ground movements.

8. CONCLUSIONS

The solutions in frequency domain are obtained by applying the linear stochastic method over a bridge under effects of the simulated earthquakes. In order to achieve proper non-stationary ground motions, more compatible parameters of the time dependent functions are considered by using approximate estimates (trial-and-error) to convergence the characteristics of the original record. The main conclusions of this paper can be drawn as:

- Soft soil site affects adversely the peak responses and the highest values develop due to the amplification of earthquakes. The soft soil condition increases the mean-peak responses up to 2.4 times and the variances up to about 7 times according to the values of the hard soil.
- Softer soil condition has produced higher peak response factors. From the analyses, the peak factors are obtained in the range of 2.88-3.29, In Vanmarcke model [17], these factors were computed as 3.45 by the quake duration of t=20 sec which is also used in this study and reliability level of 95 percent. Peak responses and variances can be limited or controlled by providing soil stiffness, modifying the rigidity of bearings or designating lengthy of piers.
- Exceedance probability functions of the peak responses are in a close relationship for the soil sets. However, the probability distributions of the soft soil decompose and display a wider dispersion even for low exceedance levels. The extreme response values significantly increase at low exceedance probabilities. Furthermore, as the exceedance probability level increases on soft soil sets, increment in response values become in exponential way like a spike in contrast to other soil types.
- Response values normalized by S1 (hard) soil results also show that the increase ratios of the peak responses corresponding to any soil type is almost constant (Table 8) for all exceedance levels. The peak responses become statistically independent from the soil types when the increase ratios are normalized by the 50 percent exceedance level values for each soil group (Table 9). Thus, if the increase ratios of any type of linear response are known for a soil site, then increase ratios of the peak responses can be predicted for the other soil types by using these known ratios.
- While time domain method requires great numbers of solutions for probabilistic responses, the frequency domain procedures yield directly. The frequency results do not only reflect the characteristics of the simulated records but also represent general solutions for expected earthquakes. Therefore, the frequency analyses can represent expected quakes other than design quake defined by courtesy of damage limitations and predetermined performance levels assigned by seismic codes.
- In case of very strong earthquakes, the isolator would most likely behave in nonlinear range and frequency domain analyses require more complex solutions including iterative procedures to consider nonlinearity.

- The peak response values obtained in this study may be used in design process or risk/reliability-based assessments for the viaduct system. However, a general inference for peak responses would require further analyses including different bridge systems.

Statements and declarations

The authors declare that they have no known competing financial interests or personal relationships that could have appeared to influence the work reported in this paper.

Conflict of interests

The authors declare no conflict of interest.

Symbols

$p(t)$	: load function
$R_p(\tau))$	: autocorrelation function
$S_p(\varpi))$	: spectral density function for load
$v(t)$	: response function
TF	: transfer function
$\{\ddot{v}\}$	: acceleration
$\{\dot{v}\}$	: displacement
$\{v\}$	: velocity
$H_n(i\varpi)$	: frequency response function
K_n	: generalized stiffness
$S_{VmVn}(\varpi)$	: cross-spectral density function
$D_{m,}$ D_n	: modal parameters
$\lvert H_g(i\varpi)\rvert$, $\lvert H_f(i\varpi)\rvert$	: filter functions
$S_x(\varpi))$	: power spectral density function for a random process
ω_g , ξ_g	: ground circular frequency and ground damping ratio
ω_f , ξ_f	: filters for the power spectrum
φ_{kr}	: random phase angle
t_{eff}	: effective duration
$z(t)$	: envelope function

$\Phi i(\varpi)$: product function

K_e, K_p, K_{eff} : initial stiffness, post-yield stiffness and effective stiffness

F_y, Q : yielding force and characteristic strength

Δ , Δ_y : rubber bearing displacement and yielding displacement

K_v : vertical stiffness.

G , A : shear modulus and rubber area

$\sum t_r$: total rubber thickness

E_c : elasticity modulus

$(\bar{x})$: mean value

σ_x : standard deviation

σ^2_x : variance

α : distribution parameter

$\ddot{V}_g(i\varpi)$: Fourier transformation

References

[1] Shinzouka, M., Jan, C.M., Digital Simulation of Random Processes and its Applications, Journal of Sound and Vibration, 22(1), 111-128, 1972.

[2] Zhu, D.Y., Zhang, Y.H., Kennedy, D., Williams, F.W., Stochastic Vibration of The Vehicle–Bridge System Subject to Nonuniform Ground Motions, Vehicle System Dynamics. 52(3), 410–428, 2014.

[3] Pagnini, L.C., Solari, G., Stochastic Analysis of The Linear Equivalent Response of Bridge Piers with Aseismic Devices, Earthquake Engineering and Structural Dynamic, 28, 543-560, 1999.

[4] Der Kiureghian A., Neuenhofer, A., A Response Spectrum Method for Multiple-Support Seismic Excitations, UCB/EERC-91/08. University of California, Berkeley, 1991.

[5] Der Kiureghian, A., Structural Response to Stationary Excitation, Journal of the Engineering Mechanics Division. 106(10), 1195-1213, 1980.

[6] Vrouwenvelder, T., Stochastic Modeling of Extreme Action Events in Structural Engineering, Probabilistic Engineering Mechanics, 15, 109-117, 2000.

[7] Yang, L.F., Leung, A.Y.T, The Stochastic Finite Segment in the Analysis of the Shear-Lag Effect on Box-Girders, Engineering Structures, 23**,** 1461-1468, 2001.

[8] Ettouney, M., Hapij, A., Gajer, R., Frequency-Domain Analysis of Long-Span Bridges Subjected to Nonuniform Seismic Motions, Journal of Bridge Engineering, 6(6), 577-586, 2001.

[9] Hasgür, Z., Stochastic Analysis of Bridge Piers with Symmetric Cantilevers under the Base Accelerations, Bulletin of the Technical University of Istanbul, 48(3-4), 657-667, 1995.

[10] Ates S., Bayraktar. A., Dumanoglu, A.A., The Effect of Spatially Varying Earthquake Ground Motions on the Stochastic Response of Bridges Isolated with Friction Pendulum Systems, Soil Dynamics and Earthquake Engineering, 26, 31-44, 2000.

[11] Jangid, R.S., Equivalent Linear Stochastic Seismic Response of Isolated Bridges, Journal of Sound and Vibration, 309**,** 805-822, 2008.

[12] Marona, G.C., Sgobba, S., Stochastic Energy Analysis of Seismic Isolated Bridges, Soil Dynamics and Earthquake Engineering, 27, 759-773, 2007.

[13] Dicleli, M., Karalar, M., Optimum Characteristic Properties of Isolators with Bilinear Force–Displacement Hysteresis for Seismic Protection of Bridges Built on Various Site Soils, Soil Dynamics and Earthquake Engineering, 31, 982–99, 2011.

[14] Sarıtaş, F., Performance-Based Seismic Assessment of a Base-isolated Bridge-pier, European Journal of Environmental and Civil Engineering, 26(1), 21-38, 2022.

[15] Sarıtaş, F., Seismic Performance Assessment of an Isolated Multispan Bridge, Arabian Journal of Science and Engineering, 47(10), 12993-13008, 2022.

[16] Qiang, H., Jianian, W., Xiuli, D., Nonlinear Response of Continuous Girder Bridges with Isolation Bearings under Bidirectional Ground Motions, Journal of Vibro engineering, 7(2), 816-826, 2015.

[17] Davenport, A.G., Note on The Distribution of Largest Values of Random Function with Application to Gust Loading, Proceedings of the Institution of Civil Engineers, 28**,** 187–196, 1964.

[18] Vanmarcke, E.H., Lomnitz, C., Rosenbleuth, E., Structural Response to Earthquakes. Chapter 8, In Seismic Risk and Engineering Decision, Elsevier, New York, USA, 1976.

[19] Mahmoud, S., Austrell, P.E., Jankowski, R., Simulation of The Response of Base-Isolated Buildings under Earthquake Excitations Considering Soil Flexibility, Earthquake Engineering and Engineering Vibration, 11(3), 359-374, 2012.

[20] Sarıtaş, F., Hasgür, Z., Dynamic Behavior of Bridge Pier with Elastomeric Bearings under Earthquake Effects for Different Soil Layers and Support Conditions, Technical Journal of Turkish Chamber of Civil Engineers, 1733-1756, 2014.

[21] Jia, H.Y., Zhang, D.Y., Zheng, S.X., Xie W.C., Pandey, M.D., Local Site Effects on a High-Pier Railway Bridge under Tridirectionally Spatial Excitations, Non-stationary Stochastic Analysis, Soil Dynamics and Earthquake Engineering, 52, 55–69, 2013.

[22] Jiao, C., Dong, X., Zhou, G.D., Wu, X.P., Seismic Response of Long-Span Triple-Tower Suspension Bridge under Random Ground Motion, Mathematical Problems in Engineering, 1-17, 2017.

[23] Adanur, S., Altunışık, A.C, Soyluk, K., Bayraktar, A., Dumanoglu, A., Contribution of Local Site-Effect on The Seismic Response of Suspension Bridges to Spatially Varying Ground Motions, Earthquakes and Structures, 10(5), 1233-1251, 2016.

[24] Schueller, G.I., Developments in stochastic structural mechanics, Archive of Applied Mechanics. **7**5(10-12) (2006) 755-773.

[25] Konaklı, K., Seismic Response Analysis with Spatially Varying Stochastic Excitation, Risk and Reliability Analysis; Theory and Applications. (Springer series in reliability engineering, 199-225, 2017.

[26] Clough R.W., Penzien, J., Dynamics of Structures, Second edition, Mc-Graw Hill Book Company, New York, 1993.

[27] Rofooei, F.R., Mobarake, A., Ahmadi, G., Generation of Artificial Earthquake Records with a Stationary Kanai-Tajimi Model, Engineering Structures, 23**,** 827-837, 2001.

[28] Kanai, K., Semi-Empirical Formula for the Seismic Characteristics of the Ground Motion, Bull Earthq. Res, Inst. University of Tokyo, 35, 309–325, 1957.

[29] Tajimi, H.A., Statistical Method of Determining the Maximum Response of a Building Structure, Proceedings of the 2nd World Conference Earthquake Engineering, 2, 1467–1482, 1960.

[30] Liu, S.C., Jhaveri, D.P., Spectral Simulation and Earthquake Site Properties, ASCE, J Eng Mech Div., 95**,** 1145–1168, 1969.

[31] Hasgür, Z., Obtaining of the Simulated Earthquake Ground Motions Depending on Soil Conditions, PhD Dissertation, Istanbul Technical University, Turkey, 1981.

[32] Penzien, J., Lee, M.C., Stochastic Analysis of Structures and Piping Systems Subjected to Stationary Multiple Support Excitations, Earthquake Engineering and Structural Dynamics. 11, 91-110, 1983.

[33] Ohsaki, Y., Introduction to Spectral Analysis of Earthquake Waves, Translated by Muzaffer İpek, TMMOB, İstanbul, Turkey, 1991.

[34] Jennings, P.C., Housner, G.W., Tsai, N.C., Simulated Earthquake Motions for Design Purposes, Proceedings of the 4th World Conference Earthquake Engineering. Chile, 1(a-1), 145–160, 1969.

[35] Housner, G.W., Jennings, P.C., Generation of Artificial Earthquakes, Probabilistic Engineering Mechanics, 90, 113-150, 1964.

[36] Şafak, E., Mueller, C., Boatwright, J., A Simple Model for Strong Ground Motions and Response Spectra, Earthquake Engineering and Structural Dynamics, 16, 203-215, 1987.

[37] Lee, S.C., Latha, V., Rajaserkan, S., Generation of Artificial Earthquake Motion Records using Wavelets and Principal Component Analysis, Journal of Earthquake Engineering, 10, 665-691, 2006.

[38] Sarıtaş, F., Stochastic Dynamic Analysis of Box-Girder Bridges, PhD Dissertation, Istanbul Technical University, Turkey, 2007.

[39] DIN 4141-14. Structural Bearings, Laminated Elastomeric Bearings Design and Construction. Deutsche Institut für Normung. 1985.

[40] AASHTO, LFRD Bridge Design Specifications, American Association of State Highway and Transportation Officials, Joints and Bearings, Washington D.C., 2007.

[41] Naeim, F. and Kelly, J.M. Design of Seismic Isolated Structure. John Wiley & Sons, U.S.A. 1999.

[42] CSI Computer & Structures Inc. SAP2000, Linear and Nonlinear Static and Dynamic Analysis of Three-Dimensional Structures. Computer & Structures, Inc., Berkeley, California. 2004.